

Lab on a Chip

Accepted Manuscript



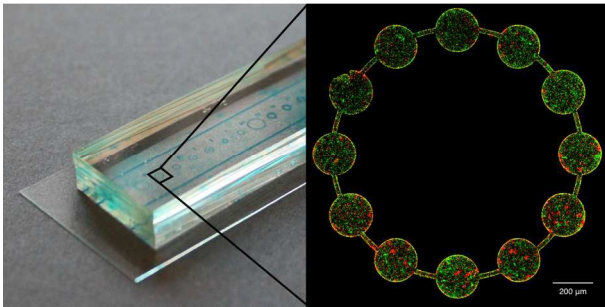
This is an *Accepted Manuscript*, which has been through the Royal Society of Chemistry peer review process and has been accepted for publication.

Accepted Manuscripts are published online shortly after acceptance, before technical editing, formatting and proof reading. Using this free service, authors can make their results available to the community, in citable form, before we publish the edited article. We will replace this *Accepted Manuscript* with the edited and formatted *Advance Article* as soon as it is available.

You can find more information about *Accepted Manuscripts* in the [Information for Authors](#).

Please note that technical editing may introduce minor changes to the text and/or graphics, which may alter content. The journal's standard [Terms & Conditions](#) and the [Ethical guidelines](#) still apply. In no event shall the Royal Society of Chemistry be held responsible for any errors or omissions in this *Accepted Manuscript* or any consequences arising from the use of any information it contains.

A simple microhabitat chip reveals the effect of patchiness on the evolution of cooperation in bacteria.



Statement of authorship: EWT, AG, ML conceived the study. EWT designed and performed the experiment. DJ and AG contributed to the chip design and fabrication. DN and AG provided the bacteria strains and guidance on experimental design. EWT wrote the first draft, and all authors contributed substantially to revisions.

Title: Patchiness in a microhabitat chip affects evolutionary dynamics of bacterial cooperation

Authors: Edward W. Tekwa^a, Dao Nguyen^b, David Juncker^c, Michel Loreau^d, Andrew Gonzalez^a

^{a.} *Department of Biology, McGill University, 1205 Dr. Penfield, Montreal, QC, H3A 1B1, Canada. E-mail: tek.wa.wong@mail.mcgill.ca*

^{b.} *Department of Medicine, McGill University, 1001 Decarie Blvd, Montreal, QC, H4A 3J1, Canada*

^{c.} *Biomedical Engineering Department, Genome Quebec Innovation Centre, and Department of Neurology and Neurosurgery, McGill University, 740 Dr. Penfield, Montreal, QC, H3A 0G1, Canada*

^{d.} *Centre for Biodiversity Theory and Modelling, Station d'Ecologie Expérimentale du CNRS, 09200, Moulis, France*

Article type: Lab on a Chip, full paper

1 **Abstract**

2 Localized interactions are predicted to favour the evolution of cooperation amongst
3 individuals within a population. One important factor that can localize interactions is
4 habitat patchiness. We hypothesize that habitats with greater patchiness (greater edge-to-
5 area ratio) can facilitate the maintenance of cooperation. This outcome is believed to be
6 particularly relevant in pathogenic microbes that can inhabit patchy habitats such as the
7 human respiratory tract. To test this hypothesis in a simple but spatially controlled setting,
8 we designed a transparent microhabitat chip (MHC) with multiple patchiness treatments at
9 the 100-micron scale. The MHC is a closed system that sustains bacterial replication and
10 survival for up to 18 hours, and allows spatial patterns and eco-evolutionary dynamics to
11 be observed undisturbed. Using the opportunistic pathogen *Pseudomonas aeruginosa*, we
12 tracked the growth of wild-type cooperators, which produce the public good pyoverdine, in
13 competition with mutant defectors or cheaters that use, but do not produce, pyoverdine. We
14 found that while defectors on average outperformed cooperators in all habitats, habitat
15 patchiness significantly alleviated the ecological pressure against cooperation due to
16 defection, leading to coexistence. Our results confirmed that habitat-level spatial
17 heterogeneity can be important for cooperation. The MHC enables novel experiments,
18 allows multiple parameters to be precisely varied and studied simultaneously, and will
19 help uncover dynamical features of spatial ecology and the evolution of pathogens.

20

21 **Keywords:** evolution of cooperation, habitat patchiness, *Pseudomonas aeruginosa*, public
22 good, microfluidic chip, pathogen, coexistence

23 1. Introduction

24 The evolution of cooperation has driven the rise of biological complexity^{1,2}. But,
25 because cooperation is costly, it is not necessarily evolutionarily viable unless the benefit of
26 cooperation tends to be directed toward cooperators. The non-uniform spatial distribution
27 of individuals is one of the most important factors favouring the evolution of cooperation³⁻
28 ¹⁰. As individuals become more clustered, the benefit of cooperation can be preferentially
29 bestowed on cooperators, making cooperation viable, either in the traditional evolutionary
30 sense —the frequency of cooperators is greater than for defectors¹¹— or in an ecological
31 sense —localized interactions are stabilizing and lead to coexistence¹²⁻¹⁴.

32 Spatial patchiness, or the ratio of edge-to-area¹⁵, characterizes the habitats of most
33 organisms¹⁶, including bacteria¹⁷. It appears that patchiness can facilitate cooperation in
34 bacteria¹⁸, likely because interactions become localized. Common bacteria such as
35 *Pseudomonas aeruginosa* are opportunistic pathogens that live in the soil¹⁹ and water²⁰,
36 and can colonize various parts of the patchy human respiratory tract²¹. The wild-type
37 bacteria are cooperators that produce the siderophore pyoverdinin, a diffusible extracellular
38 iron-chelator responsible for bacterial iron uptake and growth²² that is a form of public
39 good. The production of a public good^{23,24}, by definition, implies an individual behaviour
40 that benefits the public or the wider population, so cooperation can have an important
41 ecological effect. Interestingly, loss-of-function mutants, or defectors, often arise in the
42 human host environment over time²⁵⁻²⁷. Thus, the evolutionary race between cooperators
43 and defectors in patchy habitats is an important case for both general eco-evolutionary
44 theory^{18,28-30} and the study of infectious diseases^{31,32}.

45 The traditional approach of emulating habitat structure and localized interaction
46 has been through serial transfers of liquid subpopulations^{29,33}. This approach imposed
47 cyclical bottlenecks on population size^{34,35} during transfers, and did not allow populations
48 to form natural aggregates, since growth occurred in a relatively large-volume of well-
49 mixed liquid. Larger beaker³⁶ and flow cell experiments³⁷ allowed for endogenous spatial
50 pattern formation, but at much larger spatial scales where whole-population census is
51 generally not feasible.

52 Various microfluidic devices^{30,38-43} have been developed to emulate patchy microbial
53 habitats, which afford the capacity to track individuals in space and time while minimizing
54 sample volumes. These devices allowed detailed investigations of microbial movement,
55 pattern formation, and interaction⁴⁴. In particular, it was observed that in comparison to
56 well-mixed test tube cultures, a microhabitat favoured the maintenance of cooperation¹⁸.
57 However, these devices did not contain a systematic variation in habitat patchiness, and
58 required substantial setup time. Building on these past innovations, we introduce a
59 microhabitat chip (MHC) that is simple to fabricate and operate, reusable, and
60 systematically varies habitat patchiness.

61 The MHC is a reusable poly(dimethyl)siloxane (PDMS) chip that contains 9 habitats
62 with varying patchiness. Patchiness was achieved by fragmenting habitats at 100-micron
63 scales. We used simplicity and functionality as guiding principles⁴⁵ to focus on acquiring
64 accurate individual-level spatiotemporal data for entire habitats. The PDMS elastomer
65 layer seals with an optical cover slip to create an enclosed environment for bacteria to
66 spatially self-organize with minimal disturbance. We investigate whether three habitat
67 patchiness treatments affect the evolution of pyoverdinin^{46,47} producers, and therefore the

68 growth and equilibrium densities of cooperators and defectors in *P. aeruginosa*. The wild-
69 type cooperators and mutant defectors were genetically engineered to emit green or red
70 fluorescence, so that their population size and spatial location can be accurately quantified
71 by confocal microscopy.

72 We performed monoculture and mixed culture experiments to ascertain whether
73 habitat patchiness affects maximum growth rates and equilibrium densities of these
74 populations. We found that while defectors on average outperformed cooperators in all
75 habitats, and are thus more likely to achieve dominance, patchiness contributed to the
76 ecological coexistence of cooperators and defectors.

77 2. Methods

78 The MHC (Fig. 1) contains 9 treatments of habitat patchiness, with each habitat
79 ranging from 1400 μm to 2670 μm in diameter, and 10 or 20 μm in depth. Each habitat
80 takes the shape of a ring or a network of patches, representing a range of continuous and
81 patchy treatments with various theoretically motivated topologies (see Fig. 2 and ESI Fig.
82 S1 for specifications). Here we focus on three treatments that transition from continuous
83 to patchy (Fig. 2), which are 10 μm deep and 0.42 mm^2 in the main habitat area. At this
84 depth, all bacteria are confined to a thin layer, which facilitates image acquisition. Habitat 1
85 represents the most continuous case, whereas habitat 2 represents an intermediary
86 between the continuous and patchy cases. A central pillar is necessary in these habitats to
87 prevent collapse due to aspect ratio constraints⁴⁸. In habitat 3, 24 \times 100 μm^2 corridors are
88 introduced between 12 circular patches (210 μm diameter) to represent a patchy case with
89 the simplest network topology (area including corridors is 0.45 mm^2). The edge-to-area
90 ratios of the habitats are 0.011, 0.015, and 0.022 μm^{-1} , which represent an approximately
91 linear increase in patchiness¹⁵. Compared to the size of *P. aeruginosa* (\sim 1 μm diameter), the
92 100-micron scale patchiness treatments in the three habitats are large. On the other hand,
93 an individual bacterium can theoretically traverse 100 μm in several seconds⁴⁹, but slows
94 down considerably in aggregates when spatially confined⁵⁰. We expect that the chosen
95 scale of patchiness treatments can affect eco-evolutionary dynamics. During experiments,
96 the three habitats run in parallel. Other habitat treatments are shown in the ESI Fig. S1, but
97 no time-series data was acquired for these because of time constraints imposed by our

98 image acquisition setup. We included these extra habitat treatments as references for
99 future users.

100 A silicon mold with two spin-coated layers (to accommodate both 10 and 20 μm
101 depth features) was produced using photolithography (McGill Nanotools Microfab).
102 Polydimethylsiloxane (Sylgard 184 PDMS, Dow Corning) was poured onto the mold, cured,
103 and detached to yield MHC replicates that are about 5 mm thick, and baked at 100°C for at
104 least 24 hours. To make the PDMS MHC hydrophilic, it was soaked in 0.01N HCl at 80°C for
105 one hour, then plasma treated (modified after ⁴¹). Finally, the MHC was autoclaved, and
106 stayed in the sterilized water at room temperature until the experiment began. The MHC
107 thus remained saturated with water, which mitigated drying during the experiment.

108 We used the common *P. aeruginosa* lab strain PAO1 as our wild-type cooperators,
109 and an isogenic *pvdA* transposon mutant⁵¹, which is defective in producing the primary
110 iron-chelating siderophore (pyoverdine), as defectors. The cooperator and defector strains
111 were transformed with plasmids that constitutively expressed either the green fluorescent
112 protein GFP (pMRP9-1⁵²) or the red mCherry (pMKB1⁵³).

113 In 8 independent experimental replicates for each of 3 culture conditions
114 (cooperator monocultures, defector monocultures, mixed cultures at 1:1 initial ratio) in the
115 MHC, the expression of GFP or mCherry in cooperators and defectors were alternated to
116 average out fluorescence-dependent growth or measurement biases. Cultures were
117 prepared overnight (16 hours) in LB media with antibiotic (250 $\mu\text{g}/\text{ml}$ carbenicillin) at
118 37°C in a shaker incubator. The overnight bacterial cultures were washed and diluted to an
119 optical density (600nm) of 0.005. The experimental media consisted of casamino acids (5g
120 with 0.005M K_2HPO_4 and 0.001M MgSO_4 per litre), 50mM NaHCO_3 and 1mg/mL human

121 apo-transferrin to create an iron-limited environment where the cooperators' pyoverdinin
122 production should be beneficial^{29,46}. 0.7 μ L of the diluted culture was pipetted onto each of
123 the habitat locations on the PDMS MHC (Fig. 1). The MHC was then carefully pressed onto a
124 cover slip (24 \times 60mm #1.5H, Schott Nexterion), and excess liquid was wiped from the sides.
125 By minimizing the amount of liquid used, the PDMS reversibly sealed to the glass for the
126 duration of the experiment without additional treatment. Three such MHCs were fitted into
127 a 30°C heat chamber (Chamlide TC, Live Cell Instrument) on the inverted robotic stage of a
128 laser scanning confocal microscope (LSM 700, Zeiss) to allow for parallel experiments (two
129 for monocultures and one for mixed culture). The chamber interior was lined with wet
130 tissue papers and water wells to maintain chip moisture. Images covering the relevant
131 habitats, with 5 z-slices covering a 20 μ m slab, were acquired every 57 minutes and 18
132 seconds (the minimum acquisition time in our case) for 20 time points (Fig. 3). After an
133 experiment, the MHC was disassembled and soaked in 70% ethanol, washed, and
134 autoclaved for reuse. Each MHC can be used at least 10 times with no noticeable
135 degradation.

136 The images were cropped to show only habitat and corridor areas (Image] 1.49). We
137 then obtained the count and position of each individual bacterium at every time point
138 (Imaris 7.6.0). Some biases were observed in comparing raw GFP and mCherry counts of
139 the same strain in monocultures, and in comparing monocultures to mixed fluorescence
140 cultures of the same strain. These biases were corrected through a calibration procedure
141 (see ESI).

142 The corrected counts were converted to densities X for each habitat, and the
143 resulting time series were fitted to logistic growth curves using least-squares maximum
144 likelihood (Matlab R2013a, Eq. 1):

$$(1) \quad \frac{dX_{i,S}}{X_{i,S} dt} = r_{i,S} (1 - X_{i,S} / K_{i,S})$$

146 For a replicate of each strain i (cooperator or defector) in each culture condition S
147 (monoculture or mixed culture), we estimated its maximum growth rate r and equilibrium
148 density K . Note that we used the parameter K not as a carrying capacity, which would not
149 make sense in a mixed culture involving both inter- and intraspecific competition and
150 cooperation. Instead, we used K as an estimate of a strain's equilibrium density, since the
151 logistic growth curve describes the trajectories of each strain well regardless of culture
152 type and the length of individual time series (Fig. 4).

153 3. Results and discussion

154 In 8 biological replicates of each habitat and culture types (two monocultures and a
155 mixed culture), bacteria replicated and survived for 12 to 18 hours. The mean initial
156 density for each experiment was $0.0019 \mu\text{m}^{-2}$ ($\text{SE}=1.9\times 10^{-4}$), and according to ANOVA there
157 was no evidence of bias between culture type ($F_{2,66}=3.0$, $p=0.055$) or between habitats
158 ($F_{1,66}=0.72$, $p=0.40$). For mixed cultures, according to ANOVA, cooperator and defector
159 initial densities were not significantly different ($F_{1,45}=0.091$, $p=0.76$) and were not
160 influenced by habitats ($F_{1,45}=0.36$, $p=0.55$), indications that the experiments started at the
161 desired 1:1 cooperator-defector ratios. All cooperator and defector populations
162 demonstrated expected growth kinetics during the experimental time frame, with evidence
163 of lag, log and stationary phases (by 10 hours, Fig. 4), characteristics of logistic growth
164 curves. The equilibrium density estimates (K) represent strain populations that range from
165 2400 (cooperators in a mixed culture) to 38000 (cooperators in a monoculture)
166 individuals, or 5.6×10^8 to 9.0×10^9 individuals per mL.

167 We found that the maximum growth rate r (ESI Fig. S3) was not significantly
168 different in all cases according to ANOVA ($F_{3,87}=2.2$, $p=0.096$ for strain and culture type
169 effect, $F_{1,87}=0.090$, $p=0.77$ for patchiness effect, and $F_{3,87}=0.23$, $p=0.88$ for interaction effect).

170 In monocultures, the equilibrium density K (ESI Fig. S4) was significantly greater for
171 cooperators than for defectors (ANOVA $F_{1,44}=22$, $p=2.9\times 10^{-5}$), but was not significantly
172 different across patchiness treatments ($F_{1,44}=0.06$, $p=0.81$); the interaction between strain
173 and patchiness was not statistically significant either ($F_{1,44}=3.2$, $p=0.081$). In other words,
174 cooperation enhanced population densities regardless of habitat patchiness. In mixed
175 cultures, K was significantly lower for cooperators than for defectors ($F_{1,43}=8.3$, $p=0.0063$),

176 but was not significantly different in terms of patchiness ($F_{1,43}=0.0024, p=0.96$) and the
177 interaction between strain and patchiness ($F_{1,44}=0.047, p=0.83$). Thus, defectors
178 significantly outperformed cooperators in all habitats, a result that was also found in well-
179 mixed test tube cultures (see ESI). This illustrates the cooperation dilemma^{24,54,55}, where
180 uniform cooperation provides the best outcome for the population, but is an evolutionarily
181 inferior strategy.

182 We can further investigate the cooperation dilemma from an ecological perspective
183 through the differences between monocultures and mixed cultures. Judging from
184 monoculture equilibrium densities alone (K_{mono}), one may expect cooperators to be
185 evolutionarily dominant over defectors (since $K_{mono,C} > K_{mono,D}$). If each strain grows in
186 mixed cultures as if in monoculture, then the ratio $2K_{mix}/K_{mono}$ for each strain should be
187 one⁵⁶. The actual ratios, computed from bootstrapping, turned out to differ from one (box
188 plots in Fig. 5). Note these ratios were plotted as estimated spreads instead of individual
189 points, since they were derived statistics from unpaired experiments (by resampling with
190 replacement the numerator and denominator 2000 times). For cooperators, $2K_{mix,C}/K_{mono,C}$
191 was less than one in all habitats, indicating that when evolutionarily challenged by
192 defectors, they did not grow as well. Conversely, for defectors, $2K_{mix,D}/K_{mono,D}$ was greater
193 than one in all habitats, meaning that they benefited from cooperators.

194 The habitat patchiness effects on the $2K_{mix}/K_{mono}$ ratios can be quantified as the
195 slopes of bootstrapped linear regressions. By repeating the regression on the ratio
196 computed from the resampling of K_{mix} and K_{mono} values with replacement 2000 times, we
197 obtained the median regression slopes (lines in Fig. 5), and obtained distributions of
198 regression slopes with which to calculate the following p values. We found that patchiness

199 does not affect the $2K_{mix,D}/K_{mono,D}$ ratio for defectors ($p=0.16$). On the other hand,
200 patchiness significantly increased the $2K_{mix,C}/K_{mono,C}$ ratio for cooperators ($p=0.0075$).
201 These trends suggest that with increased patchiness, the ecological pressure against the
202 pyoverdin public good cooperation, stemming from the challenge by defectors, is alleviated.
203 Moreover, as patchiness increases, the ratios $2K_{mix,C}/K_{mono,C}$ and $2K_{mix,D}/K_{mono,D}$ appear to
204 approach one, so patchiness leads competing strains to grow as if in isolation. This effect is
205 known in ecology as a spatial stabilizing effect, in that patchiness isolates strains such that
206 they increasingly compete within strains rather than between strains, leading to
207 coexistence regardless of how competitive each strain is relative to the other¹²⁻¹⁴.

208 Our experiment generated the first empirical evidence that a gradual increase in
209 habitat patchiness, occurring at a scale much larger than the individual, can affect the
210 ecology of cooperation, and the coexistence of cooperators and defectors in bacteria. These
211 results complement a previous microfluidic experiment¹⁸, which demonstrated the
212 coexistence of bacterial cooperators and defectors in one microhabitat. The results are
213 comparable to traditional test tube experiments, which by controlling serial transfer
214 patterns, showed that spatial restrictions and artificially localized interactions can favour
215 the evolution of cooperation^{29,33-35}. Our MHC also provides an alternative to beaker³⁶ and
216 flow cell experiments³⁷, which study cooperative aggregates and biofilms at much larger
217 spatial scales where whole-population census is generally not feasible.

218 We have overcome important challenges that are crucial for the use of microscale
219 habitat devices in evolutionary biology. The major obstacles to a wider uptake of
220 microfluidic technologies are costly start-up equipment, complicated setup, and associated
221 risks of error and contamination⁴⁵, complexities that are not always geared to answer basic

222 but outstanding eco-evolutionary questions. In creating a sealed chip that can run multiple
223 replicates without pumps for 12-18 hours, we have enabled high-throughput spatial
224 experiments with minimal setup time and cost. The runtime is an improvement over
225 previous PDMS microhabitat devices^{38,39}, and is much simpler to operate than devices
226 requiring active nutrient flow^{30,40-42}. Many aspects of the generated data, such as
227 individual positions, population spatial distributions, and movement patterns can be
228 further investigated, and would lead to a more comprehensive understanding of patchiness
229 and individual-level clustering effects^{57,58} than what our current analyses yielded. It is also
230 possible to recover bacteria from the MHC at the end of experiments to detect *de novo*
231 mutations through sequencing⁴². The simplicity of the MHC greatly facilitates running an
232 entire eco-evolutionary experiment on a chip.

233 Some limitations exist with the MHC. Because of aspect ratio requirements with
234 PDMS chambers⁴⁸, it is not possible to create patches and habitats of any dimension. The
235 enclosed system afforded by our design is simple and exhibits the familiar logistic growth
236 of bacteria (Fig. 4). However, without serial transfer of bacteria into fresh medium, the
237 system limits the possible duration of the experiment for the following reasons. PDMS
238 facilitates gas exchange, but gradually absorbs liquid at the same time⁵⁹. The sealed system
239 also prevents nutrients from being replenished, but conversely minimizes the risks of
240 external contamination. Lastly, the number of different strains that can be tracked
241 simultaneously was limited by the number of fluorescent proteins (eg. GFP, mCherry)
242 distinguishable using our current setup, but additional fluorescent proteins are available⁶⁰.

243 4. Conclusions

244 We demonstrated that a simple and reusable microfluidic chip can provide insights
245 into the eco-evolutionary dynamics of *Pseudomonas aeruginosa*, a medically important
246 pathogen. In the first microbial cooperation experiment with multiple spatial habitat
247 treatments, we observed that mutant defectors are evolutionarily more competitive than
248 wild-type cooperators that produce siderophores. However, the ecological pressure
249 against cooperation due to defection is alleviated in increasingly patchy habitats, leading to
250 continued coexistence (Fig. 5). The trends suggest that at patchiness levels higher than
251 those we tested, competing strains may grow as if in isolation – a hypothesis that merits
252 further investigations.

253 The results suggest that pathogenic bacteria in patchy habitats, such as the
254 respiratory tract²¹, may be more cooperative in exploiting nutrient resources in
255 comparison to a continuous habitat like a conventional test tube. Nevertheless, defectors,
256 or loss-of-function mutants, can be expected to arise and co-exist with wild-type
257 cooperators, as has been observed in patients with cystic fibrosis²⁵⁻²⁷. The simple chip
258 design and operation should facilitate its uptake in ecological, evolutionary, and medical
259 research, leading to novel experiments that complement existing studies on microbes in
260 spatially complex environments^{18,29,37,42,61}. Specifically, future experiments using our
261 microhabitat chip can address how habitat patch size and corridor topology affect
262 demography⁶²⁻⁶⁴ and cooperation^{5,65}, and how nutrient availability⁶⁶ interacts with
263 patchiness to affect microbial community dynamics⁶⁷.

264 **Acknowledgements**

265 EWT was supported by the Fonds Québécois de la Recherche sur la Nature et les
266 Technologies and the Québec Centre for Biodiversity Science. ML was supported by the
267 TULIP Laboratory of Excellence (ANR-10-LABX-41). AG and DJ were supported by the
268 Canada Research Chair program and NSERC Discovery grants. DN was supported by a CFI
269 Leaders Opportunity Fund (25636), a Burroughs Wellcome Fund CAMS award
270 (1006827.01) and a CIHR salary award. M. Nannini created the silicon mold for the chip.
271 G.A. McKay helped creating the GFP and mCherry strains in the study, and provided
272 experimental guidance. We would like to thank M.R. Parsek and S. Moskowitz for
273 generously providing the pMRP9-1 and pMKB1 plasmids, respectively.

274 **References**

- 275 1. J. Maynard Smith and E. Szathmáry, *The origins of life*, Oxford University Press,
276 Oxford, 1999.
- 277 2. W. D. Hamilton, *J. Theor. Biol.*, 1964, **7**, 1–16.
- 278 3. S. Lion and M. van Baalen, *Ecol. Lett.*, 2008, **11**, 277–295.
- 279 4. J. A. Fletcher and M. Doebeli, *Proc. R. Soc. B Biol. Sci.*, 2009, **276**, 13–9.
- 280 5. C. E. Tarnita, H. Ohtsuki, T. Antal, F. Fu, and M. A. Nowak, *J. Theor. Biol.*, 2009, **259**,
281 570–81.
- 282 6. F. Débarre, C. Hauert, and M. Doebeli, *Nat. Commun.*, 2014, **5**, 3409.
- 283 7. D. S. Wilson, *Am. Nat.*, 1977, **111**, 157–185.
- 284 8. F. Rousset, *Genetic Structure and Selection in Subdivided Populations*, Princeton
285 University Press, Princeton, NJ, 2004.
- 286 9. A. Gardner and S. A. West, *J. Evol. Biol.*, 2004, **17**, 1195–1203.
- 287 10. H. Celiker and J. Gore, *Trends Cell Biol.*, 2013, **23**, 9–15.
- 288 11. S. H. Rice, *Evolutionary Theory*, Sinauer, Sunderland, MA, 2004.
- 289 12. S. A. Levin, *Am. Nat.*, 1974, **108**, 207–228.
- 290 13. B. M. Bolker and S. W. Pacala, *Am. Nat.*, 1999, **153**, 575–602.
- 291 14. P. Chesson, *Annu. Rev. Ecol. Syst.*, 2000, **31**, 343–366.
- 292 15. P. A. Marquet, M.-J. Fortin, J. Pineda, D. O. Wallin, J. Clark, Y. Wu, S. Bollens, C. M.
293 Jacobi, and R. D. Holt, in *Patch dynamics*, eds. S. A. Levin, T. M. Powell, and J. H. Steele,
294 Springer-Verlag, New York, 1993, pp. 277–304.
- 295 16. S. a. Levin, *Ecology*, 1992, **73**, 1943–1967.
- 296 17. C. H. Ettema and D. a. Wardle, *Trends Ecol. Evol.*, 2002, **17**, 177–183.
- 297 18. F. J. H. Hol, P. Galajda, K. Nagy, R. G. Woolthuis, C. Dekker, and J. E. Keymer, *PLoS One*,
298 2013, **8**, e77402.

- 299 19. S. K. Green, M. N. Schroth, J. J. Cho, S. K. Kominos, and V. B. Vitanza-jack, *Appl.*
300 *Microbiol.*, 1974, **28**, 987–991.
- 301 20. K. Botzenhart and G. Döring, in *Pseudomonas aeruginosa as an Opportunistic*
302 *Pathogen*, Springer US, 1993, pp. 1–18.
- 303 21. A. Folkesson, L. Jelsbak, L. Yang, H. K. Johansen, O. Ciofu, N. Høiby, and S. Molin, *Nat.*
304 *Rev. Microbiol.*, 2012, **10**, 841–851.
- 305 22. K. Poole and G. A. McKay, *Front. Biosci.*, 2003, **8**, 661–686.
- 306 23. M. Olson, *The Logic of Collective Action*, Harvard University Press, Harvard, MA, 1965.
- 307 24. E. Ostrom, *J. Econ. Perspect.*, 2000, **14**, 137–158.
- 308 25. D. De Vos, M. De Chial, C. Cochez, S. Jansen, B. Tümmler, J. M. Meyer, and P. Cornelis,
309 *Arch. Microbiol.*, 2001, **175**, 384–388.
- 310 26. E. E. Smith, D. G. Buckley, Z. Wu, C. Saenphimmachak, L. R. Hoffman, D. a D’Argenio, S.
311 I. Miller, B. W. Ramsey, D. P. Speert, S. M. Moskowitz, J. L. Burns, R. Kaul, and M. V
312 Olson, *Proc. Natl. Acad. Sci. U. S. A.*, 2006, **103**, 8487–8492.
- 313 27. D. Nguyen and P. K. Singh, *Proc. Natl. Acad. Sci. U. S. A.*, 2006, **103**, 8305–8306.
- 314 28. J. Smith, J. D. Van Dyken, and P. C. Zee, *Science*, 2010, **328**, 1700–1703.
- 315 29. A. S. Griffin, S. A. West, and A. Buckling, *Nature*, 2004, **430**, 1024–7.
- 316 30. J. E. Keymer, P. Galajda, G. Lambert, D. Liao, and R. H. Austin, *Proc. Natl. Acad. Sci. U. S.*
317 *A.*, 2008, **105**, 20269–73.
- 318 31. B. Crespi, K. Foster, and F. Úbeda, *Philos. Trans. R. Soc. Lond. B. Biol. Sci.*, 2014, **369**,
319 20130366.
- 320 32. A. Buckling, F. Harrison, M. Vos, M. a Brockhurst, A. Gardner, S. a West, and A. Griffin,
321 *FEMS Microbiol. Ecol.*, 2007, **62**, 135–141.
- 322 33. R. Kümmerli, A. Gardner, S. a West, and A. S. Griffin, *Evolution*, 2009, **63**, 939–949.
- 323 34. M. a Brockhurst, *PLoS One*, 2007, **2**, e634.
- 324 35. J. S. Chuang, O. Rivoire, and S. Leibler, *Science*, 2009, **323**, 272–275.
- 325 36. P. B. Rainey and K. Rainey, *Nature*, 2003, **425**, 72–74.
- 326 37. C. D. Nadell, J. B. Xavier, and K. R. Foster, *FEMS Microbiol. Rev.*, 2009, **33**, 206–224.

- 327 38. S. Park, P. M. Wolanin, E. a Yuzbashyan, P. Silberzan, J. B. Stock, and R. H. Austin,
328 *Science*, 2003, **301**, 188.
- 329 39. S. Park, P. M. Wolanin, E. a Yuzbashyan, H. Lin, N. C. Darnton, J. B. Stock, P. Silberzan,
330 and R. Austin, *Proc. Natl. Acad. Sci. U. S. A.*, 2003, **100**, 13910–13915.
- 331 40. A. Groisman, C. Lobo, H. Cho, J. K. Campbell, Y. S. Dufour, A. M. Stevens, and A.
332 Levchenko, *Nat. Methods*, 2005, **2**, 685–689.
- 333 41. H. Cho, H. Jönsson, K. Campbell, P. Melke, J. W. Williams, B. Jedynek, A. M. Stevens, A.
334 Groisman, and A. Levchenko, *PLoS Biol.*, 2007, **5**, e302.
- 335 42. Q. Zhang, G. Lambert, D. Liao, H. Kim, K. Robin, C. Tung, N. Pourmand, and R. H.
336 Austin, *Science*, 2011, **333**, 1764–1767.
- 337 43. A. K. Wessel, T. a Arshad, M. Fitzpatrick, J. L. Connell, R. T. Bonnecaze, J. B. Shear, and
338 M. Whiteley, *MBio*, 2014, **5**, e00992–14.
- 339 44. R. H. Austin, C.-K. Tung, G. Lambert, D. Liao, and X. Gong, *Chem. Soc. Rev.*, 2010, **39**,
340 1049–1059.
- 341 45. E. K. Sackmann, A. L. Fulton, and D. J. Beebe, *Nature*, 2014, **507**, 181–189.
- 342 46. J. M. Meyer, a Neely, a Stintzi, C. Georges, and I. a Holder, *Infect. Immun.*, 1996, **64**,
343 518–523.
- 344 47. S. A. West and A. Buckling, *Proc. Biol. Sci.*, 2003, **270**, 37–44.
- 345 48. Y. Xia and G. M. Whitesides, *Annu. Rev. Mater. Sci.*, 1998, **28**, 153–184.
- 346 49. T. B. Doyle, A. C. Hawkins, and L. L. McCarter, *J. Bacteriol.*, 2004, **186**, 6341–6350.
- 347 50. J. L. Connell, A. K. Wessel, M. R. Parsek, A. D. Ellington, M. Whiteley, and J. B. Shear,
348 *MBio*, 2010, **1**, e00202–10.
- 349 51. K. Held, E. Ramage, M. Jacobs, L. Gallagher, and C. Manoil, *J. Bacteriol.*, 2012, **194**,
350 6387–6389.
- 351 52. D. G. Davies, M. R. Parsek, J. P. Pearson, B. H. Iglewski, J. W. Costerton, and E. P.
352 Greenberg, *Science*, 1998, **280**, 295–298.
- 353 53. M. K. Brannon, J. M. Davis, J. R. Mathias, C. J. Hall, J. C. Emerson, P. S. Crosier, A.
354 Huttenlocher, L. Ramakrishnan, and S. M. Moskowitz, *Cell. Microbiol.*, 2009, **11**, 755–
355 768.
- 356 54. T. Killingback, M. Doebeli, and C. Hauert, *Biol. Theory*, 2010, **5**, 3–6.

- 357 55. G. Hardin, *Science*, 1968, **162**, 1243–1248.
- 358 56. B. J. Cardinale, J. P. Wright, M. W. Cadotte, I. T. Carroll, A. Hector, D. S. Srivastava, M.
359 Loreau, and J. J. Weis, *Proc. Natl. Acad. Sci. U. S. A.*, 2007, **104**, 18123–18128.
- 360 57. S. A. Levin and S. W. Pacala, in *Spatial ecology: the role of space in population*
361 *dynamics and interspecific interactions*, eds. D. Tilman and P. Kareiva, Princeton
362 University Press, Princeton, NJ, 1997, pp. 271–296.
- 363 58. S. A. Levin, *Bioscience*, 2005, **55**, 1075–1079.
- 364 59. M. W. Toepke and D. J. Beebe, *Lab Chip*, 2006, **6**, 1484–1486.
- 365 60. L. Yang, M. Nilsson, M. Gjermansen, M. Givskov, and T. Tolker-Nielsen, *Mol. Microbiol.*,
366 2009, **74**, 1380–1392.
- 367 61. G. Bell and A. Gonzalez, *Science*, 2011, **332**, 1327–1330.
- 368 62. I. Hanski, *Nature*, 1998, **396**, 41–49.
- 369 63. A. Gonzalez, J. Lawton, F. Gilbert, T. Blackburn, and I. Evans-Freke, *Science*, 1998,
370 **281**, 2045–7.
- 371 64. E. I. Damschen, L. a Brudvig, N. M. Haddad, D. J. Levey, J. L. Orrock, and J. J.
372 Tewksbury, *Proc. Natl. Acad. Sci. U. S. A.*, 2008, **105**, 19078–19083.
- 373 65. P. D. Taylor, T. Day, and G. Wild, *Nature*, 2007, **447**, 469–472.
- 374 66. S. Kéfi, M. van Baalen, M. Rietkerk, and M. Loreau, *Am. Nat.*, 2008, **172**, E1–17.
- 375 67. M. a. Leibold, M. Holyoak, N. Mouquet, P. Amarasekare, J. M. Chase, M. F. Hoopes, R. D.
376 Holt, J. B. Shurin, R. Law, D. Tilman, M. Loreau, and a. Gonzalez, *Ecol. Lett.*, 2004, **7**,
377 601–613.

378

Figures

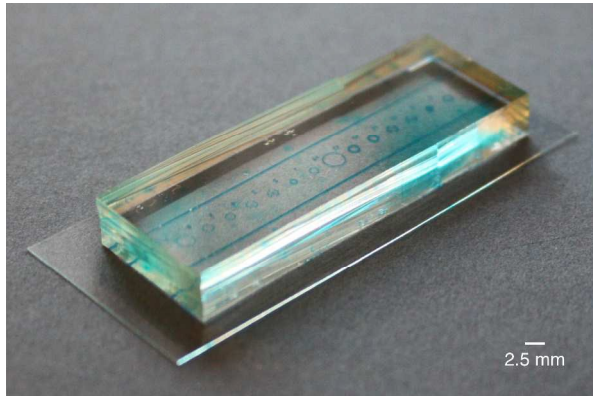


Figure 1. The microfluidic device contains 14 habitats and 9 variations (some are duplicated). Habitats were dyed blue for visualization. The elastomer (PDMS) layer was pressed onto a 60 mm x 24 mm glass cover slip after inoculation to create a sealed device. The confocal microscope acquired images through the thin cover slip.

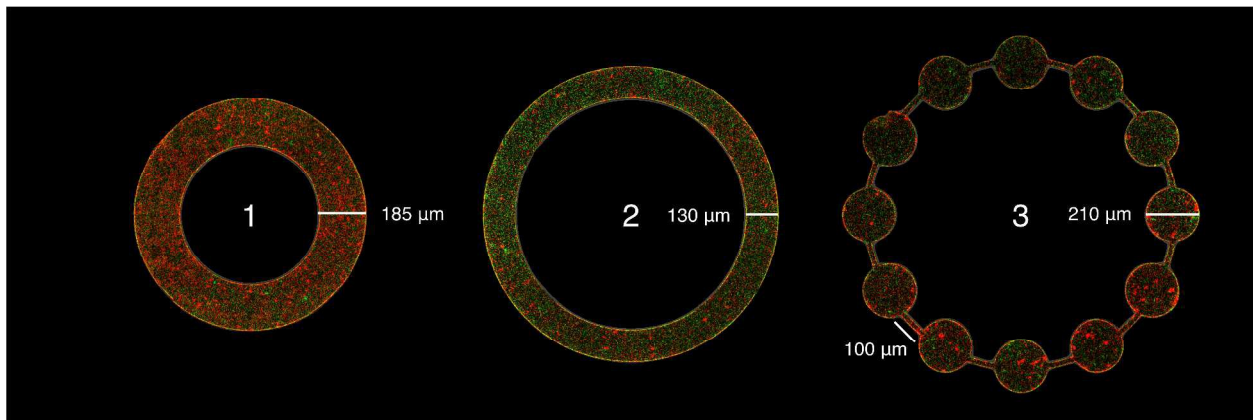


Figure 2. Three habitat patchiness treatments. The habitats were inoculated with green cooperators and red defectors. Images shown were taken at $T=10$ (about 10 hours after inoculation). The habitats are 10 μm deep and have diameters of 915, 1165 and 1405 μm . The corridors are 24 μm wide. The habitat areas are 0.42, 0.42, and 0.45 mm^2 . The edge-to-area ratios, or patchiness measures, are 0.011, 0.015, and 0.022 μm^{-1} .

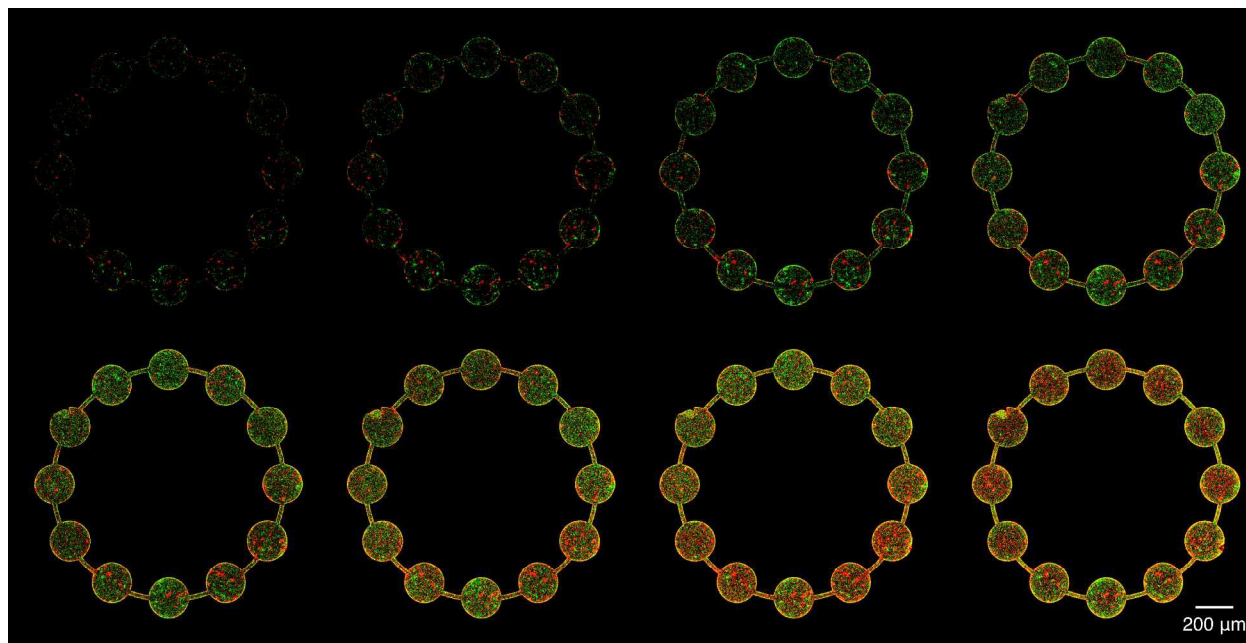


Figure 3. Timed images of green cooperators and red defectors in a patchy habitat (T=5 to 12 from top left to bottom right). For all figures, the time interval T is 57 minutes 18 seconds.

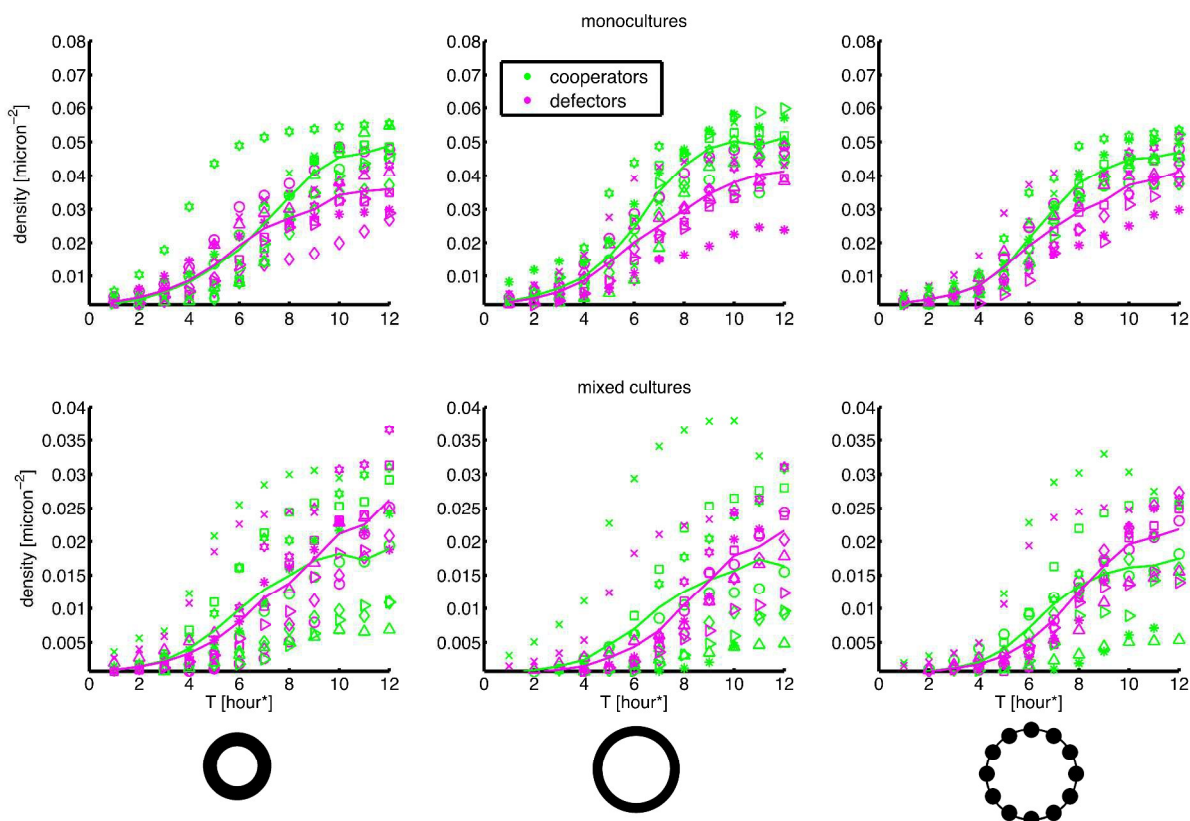


Figure 4. Time series of cooperator and defector monocultures, and mixed cultures in three habitat patchiness treatments, as illustrated by icons at the bottom. Densities are expressed as individuals per micron squared. The different markers represent the 8 experimental replicates, and the line plots are averages for each strain at each time point. *Each time interval T is 57 minutes 18 seconds.

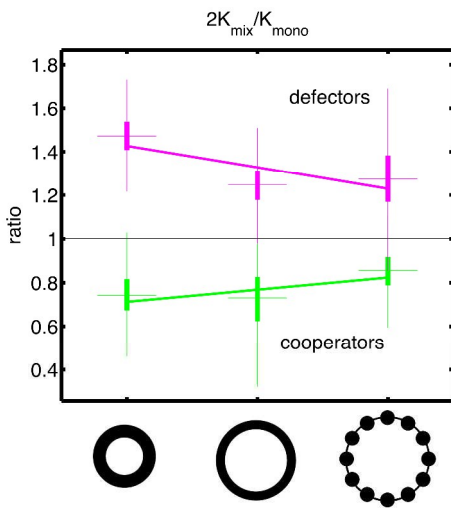


Figure 5. The ratios of equilibrium densities (K) in mixed cultures ($\times 2$) over monocultures as estimated from bootstrapping for three habitats. If the interaction between cooperators and defectors has no effect on their equilibrium densities, the ratio should be 1. In the box plots, horizontal bars indicate medians, thick vertical bars (boxes) indicate 25th and 75th percentiles, and thin vertical bars indicate minima and maxima excluding outliers. From bootstrapped linear regressions, patchiness significantly increased the ratio for cooperators (green regression line, $p=0.0075$), but marginally decreased the ratio for defectors (magenta regression line, $p=0.16$).